Magnetic zones of Mars: Deformation controlled origin of magnetic anomalies

Gunther Kletetschka[1, 2, 3], Rob Lillis[4], N. F. Ness[1,5], M. H. Acuña[3], J. E. P. Connerney[3], and Peter J. Wasilewski[3]

[1] Department of Physics, Catholic University of America, Washington D.C., USA
[2] Institute of Geology, Academy of Sciences, Prague, Czech Republic
[3] NASA Goddard Space Flight Center, Greenbelt, Maryland, USA
[4] Space Sciences Laboratory, UC Berkeley, Berkeley, California, USA
[5] Bartol Research Institute, University of Delaware, Newark, Delaware, USA

Abstract:

Intense magnetic anomalies over the Mars surface suggest preservation of large volumes of very old crust (>3 By) that formed in the presence of global magnetic field. The global distribution of the magnetic intensities observed above the Mars crust suggests a division into three zones. Zone 1 is where the magnetic signature is negligible or of relatively low intensity at Mars Global Surveyor (MGS) satellite mapping altitude (400 km). Zone 2 is the region of intermediate crustal magnetic amplitudes and Zone 3 is where the highest magnetic intensities are measured. Crater demagnetization near Zone 3 reveals the presence of rocks with both high magnetic intensity and coercivity. Magnetic analyses of terrestrial rocks show that compositional banding in orogenic zones significantly enhances both magnetic coercivity and thermal remanent magnetization (TRM) efficiency. Such enhancement offers a novel explanation for the anomalously large intensities inferred of magnetic sources on Mars. We propose that both large magnetic coercivity and intensity near the South Pole is indicative of the presence of a large degree of deformation. Associated compositional zoning creates conditions for large scale magnetic anisotropy allowing magnetic minerals to acquire magnetization more efficiently, thereby causing the distinct magnetic signatures in Zone 3, expressed by intense magnetic anomalies. We use a simple model to verify the magnetic enhancement. We hypothesize that magnetically enhanced zone would reside over the down welling plume at the time of magnetization acquisition.

Introduction

The discovery of intense magnetic anomalies on Mars by Mars Global Surveyor (MGS) (Acuna et al., 1999; Connerney et al., 1999) emphasizes that magnetism must play an important role during the early formation of planets. Cratering events constrain these anomalies to have been formed during the very early phase of Mars evolution covering the first several hundred millions of years (Acuna et al., 1999). However, it has been argued, based on models of core cooling and presence of significant magnetic field values over the northern lowlands and underneath portions of Tharsis region, that the dynamo may have persisted beyond the first 500 Myr (Schubert et al., 2000; Stevenson et al., 1983). After its cessation, all new crust would be formed with little or no magnetization (magnetization by existing crustal fields should be negligible (Arkani-Hamed, 2003)

unless significant concentration of magnetic minerals allows for magnetic interaction and enhancement of magnetic anomalies (Kletetschka et al., 2005).
The ~400 km-altitude map of radial magnetic field of Connerney et al. (2001) can be used to outline three prominent zones 1, 2 and 3, separating the Martian crust into regions above which the magnetic fields of crustal origin are weak, intermediate and strong, respectively (Figure 1). Magnetic anomalies near the impact basins Argyre (1000 km), Hellas (1520 km), and Isidis (1200 km) are likely to be caused by minerals with low to moderate magnetic coercivity. This is due to preferential impact demagnetization of the minerals with low coercivity. Low coercivity minerals are characterized be larger extent of demagnetization of preexisting magnetic anomalies. This has been verified experimentally and numerically. Magnetic anomalies vanish near the impact basins and the crustal magnetic coercivity controls the rate of magnetic decay near the basins (Kletetschka et al., 2004b). Figure 1 shows that these craters are within Zone 1 and adjacent to Zone 2. There is an exception, however. The Prometheus basin (860 km) straddles the boundary of Zone 3 (Figure 2) and therefore the magnetic anomaly decay near this basin is critical for characterization of the magnetic carriers in this region. In fact, the steep magnetic decay towards the center of the Prometheus basin suggests that the crustal magnetic minerals most likely have large magnetic coercivity (Kletetschka et al., 2004b).

Prometheus basin is 860 km in diameter, and is within the diameter range of large impact basins on Mars (1000 km, 1200 km, and 1520 km for Argyre, Isidis, and Hellas impact basins respectively). The nature of magnetic anomalies distribution near Prometheus is very different compared with other large impact basins (Figure 2, and Figure 1 in (Kletetschka et al., 2004b)). Note that there is an unaccounted absence of magnetic anomalies (which could be due to smaller block sizes containing coherent magnetization) around its basin. However the presence of strong anomalies in proximity of this basin reveals a resistance against impact demagnetization supporting large crustal magnetic coercivity (Kletetschka et al., 2004b). The pressure gradient that must have occurred during the impact event was estimated while considering the impact basin diameter and the evidence of presence of large magnetic anomalies indicates anomalous resistance against impact demagnetization - large crustal magnetic coercivity.

New experiments testing nature of thermal remanence acquisition

The investigation of TRM (Thermal remanent magnetization) of rocks and minerals (Dunlop and Özdemir, 1997) has focused on expressions of TRM of highly shaped magnetic minerals. It has been shown recently (Kletetschka et al., 2004a) that magnetic elongation beyond 1/5 aspect ratio results in significantly enhanced TRM/SIRM (Saturation Isothermal Remanent Magnetization) acquisition. Besides the large sensitivity of magnetic acquisition to shape of the grains, which appears to be similar across different minerals, note that TRM/SIRM conserves even for different grain sizes when in equidimensional shape (Kletetschka et al., 2004a). However, note that single domain grain sizes TRM/SIRM ratio can be larger by factor of two (Yu, 2006) than when minerals are in pseudosingle domain state or multidomain state. Factor of two, enlargement, is much less comparing to the enlargement due to grain elongation of fabric

elongation as mentioned further. Moreover, work by Yu presents data for magnetite only and thus this observation may not be generalized to all magnetic minerals.

Extreme shapes of magnetic minerals are significantly lowering their demagnetizing factor causing them to be highly efficient in acquiring any magnetization. We decided to test two cases (Case 1 and Case 2) that may be relevant to deformation on Mars. Case1: Samples consist of mineral containing elongated magnetic grains as inclusions. We selected an Archean annorthosite containing highly stretched oxide (magnetite – we will provide the evidence further) inclusions (up to 1/50 aspect ratio). Samples used in the present study were collected in the Middle and Upper Banded Series of the Stillwater Complex, a large (~ 180 km^2 exposed), ultramafic to anorthositic intrusion at the edge of the Wyoming Craton in Montana, USA (Selkin et al., 2000) Large aspect ration results in magnetic coercivity near 50 mT as seen in hysteresis properties (see Figure 3 in (Selkin et al., 2000)). Case 2: We located samples with a high degree of separation between denser and lighter minerals forming visible bands (gneiss). Samples were selected from highly metamorphosed rocks (granulites and gneisses) from the Kohistan arc, a collision zone, which forms boundary of highly deformed rocks between Asia and India plates (Schlinger et al., 1989). The southern boundary of the Kohistan arc is a northward dipping thrust on which the southern parts of the Kohistan arc have been thrust over India (Bard, 1983).

Case 1: The anorthosite samples contained oxide needles that were recognized by magnetic anisotropy measurements (Selkin et al., 2000). Transmission electron microscopy showed that the stretched oxides have aspect ratio of these needles as large as 1/50 (Xu et al., 1997). These samples were tested for efficiency of acquisition of TRM. The elongation of the grains enhanced TRM normalized by saturation isothermal remanence up to the values 0.30-0.70. This is significantly higher that the same ratio reported on TRM of equi-dimensional grains with the TRM/SIRM range 0.007-0.020 (Kletetschka et al., 2006) or in another independent study, supporting the empirical law, where the TRM/SIRM ratio of either SD or MD equi-dimensional grains is within the range 0.03-0.05 (Yu, 2007). Cryogenic test of stability of magnetic remanence revealed magnetic transition near 120K (Figure 3a), which is also known as the Verwey transition (Verwey et al., 1947). This transition is characteristic for magnetite when the easy axis of magnetization changes from 111 to 100. Magnetic enhancement of TRM/SIRM is shown in Figure 3b where TRM/SIRM increased in respect the TRM/SIRM predicted by empirical law (Kletetschka et al., 2004a; Kletetschka et al., 2006).

Case 2: Samples from Kohistan have a variety of deformations. From the suite of rocks across the subduction zone some contain various degrees of mafic band formation. These samples we exposed in outcrops along the Karakoram highway (Pakistan) within repetition of shear zones and zones with no apparent deformation. We selected four rock specimens (Figure 4) with both homogeneous texture (no fabric present) and four specimens with well-developed fabric present (separation of mafic minerals into planes in approximate aspect ratio 1/6). Each pair of deformed and un-deformed rock was adjacent to each other. Both groups of samples were subjected to TRM acquisition in 0.05 mT external field, simulating the geomagnetic field. Samples with fabric showed significantly higher remanence efficiency (TRM/SIRM) than the sample without fabric present (SIRM at 3T).

Our experiments showed that thermal acquisition of remanence is greatly enhanced when the magnetic mineral is highly elongated. TRM experiments on rock

specimens from Kohistan, where minerals are not necessarily elongated but clustered into planar bands, revealed a less spectacular but still significantly larger TRM (factor of 2-5 comparing to equidimensional grains). This observation offers one possibility for interpretation of the intensely magnetized Mars crust: enhanced magnetization via large-scale magnetic anisotropy.

We attempted to model this behavior (see Figure 5) with magnetic simulation software "Finite Element Method Magnetics" written by David Meeker and freely available at http://femm.berlios.de. Magnetic crust is modeled with crustal blocks 50kmx50km in size. Magnetization oscillates from block to block and is either up or down as shown in Figure 5 by white arrows. Block with no (or horizontal) fabric has magnetization 60 A/m while the block with elongated vertical fabric has magnetization of 300 A/m. This is factor 5 more than magnetization generated by blocks with no fabric and this can account for large-scale magnetic anisotropy that may exist within these blocks. These magnetizations relate to 0.6% and 3% of dispersed single domain magnetite in non magnetic matrix, respectively (see (Kletetschka et al., 2000)). In order to enhance the TRM of the magnetic carriers 5 times like shown in this model the aspect ratio of the magnetic carriers needs to be between 1/10-1/15 based on the TRM/SIRM trends (Figure 4c). Magnetizations from the anisotropic blocks in this model generate magnetic anomaly intensities similar to the ones observed by Mars Global Surveyor (Figure 1). The combination of the 50 km blocks into larger scale bodies generates large-scale anomaly observable at satellite altitude. The maximum effect is at the transition from one type of magnetized body into another, where the blocks are comparable to the satellite altitude.

Our model (Figure 5) assumes crustal thickness 50 km. Other authors assumed sources near 100 km deep (Arkani-Hamed, 2002; Nimmo and Gilmore, 2001), however the thickness, magnetization intensity, and source depth are poorly constrained observationally (Connerney et al., 2004). When considering larger thicknesses (>50 km) we may not need magnetization as large as 300 A/m. The main point that we want to illustrate is that the 5 fold enhancement of one block due to anisotropy can generate large magnetization contrasts observable at satellite altitude.

Discussion:

Figure 1 shows that crustal magnetic fields on Mars can be classified into three regions, characterized by increasing signal amplitude at satellite altitude: small, medium and large. Following are four possible explanations, outlined below as Explanation A,B,C,D:

Explanation A. Magnetization intensity correlated with iron content, i.e., Zone 3 has more iron content than zones 2 and even more than zone 1. Iron is present in paramagnetic and mutlidomain minerals.

Explanation B: Remanent magnetization correlated with volume fraction of magnetic minerals, i.e., Zone 3 has more remanent magnetic minerals than zones 2 and even more than zone 1.

Explanation C. Universally magnetized crust that has been reworked, or remagnetized in a low field environment, i.e., initially all zones were magnetized to the same degree. Then zones 1 and 2 were demagnetized (zone 1 more efficiently) by impact events or due to heat from volcanic events.

Explanation D. Variations in crustal magnetic fields attributed to efficiency of magnetization. Zone 3 was magnetized more efficiently than zones 2 and even more efficiently than zone 1.

There is no significant density correlation with intense magnetic anomalies (Neumann et al., 2004). We still cannot dismiss A. This is partly because Mars has no global magnetic field and therefore there is negligible contribution from the induced magnetization. Induced magnetization depends on the volumetric content of magnetic mineral and therefore magnetic anomalies due to induced magnetization are more likely to correlate with iron content as oppose to magnetic anomalies generated by remanent magnetization (Mars magnetic anomalies).

Explanation B would be a region where the intense magnetic anomalies are caused by overwhelming precipitation of magnetic mineral (e.g magnetite) under the presence of coherent non-changing magnetic field. Such magnetic minerals have to be able to carry a stable magnetic remanence of various direction and intensity, depending on the history of the rock hosting these minerals and in general may enhance or reduce magnetic anomaly independently of the concentration of magnetic carriers. This may be the case of serpentinization – oxidation of olivine rich basalt results in serpentine and magnetite precipitates (Quesnel et al., 2007; Rasmussen et al., 2006) or thermal decomposition of iron rich carbonates (Scott and Fuller, 2004) where water reacting with ancient Martian atmospheric carbon dioxide dissolves igneous rocks in the crust and precipitate iron rich carbonates as observed in Martian meteorites. Thermal decomposition of these rocks generates plentiful single domain magnetite, causing the magnetic anomalies if precipitated during the presence of global magnetic field.

Explanation C has drawn considerable discussion since there is a lack of magnetic intensity over the large impact basins (Acuna et al., 1999; Kletetschka et al., 2004b; Mohit and Arkani-Hamed, 2004). This may be due to shock demagnetization of magnetic minerals; even small impacts can significantly demagnetize even high coercivity minerals (Kletetschka et al., 2004b). Pyrrhotite was thought to be least stable during impact conditions (Rochette et al., 2003); however, impact magnetization stability of pyrrhotite was disputed to be higher (Louzada et al., 2007). Shock demagnetization of minerals can explain lower magnetic anomaly intensity over zone 1. Lack of magnetization is correlated with the large impacts and volcanic provinces. Further research argued (Connerney et al., 2005) that large regions of the Mars crust were partially or completely demagnetized by emplacement of single-cooling event lavas, e.g., northern plains (Utopia, Isidis) and the prominent volcanic provinces (Tharsis, Elysium, Olympus Mons, Alba Patera).

Explanation D, efficiency of magnetization, really consists of two distinct possibilities: The first involves the efficiency of magnetization of a particular mineral, whereas the second involves only the volume (block size) of coherent magnetization. Homogeneously magnetized volume determines the distance (altitude) from which the magnetization can be most efficiently recognized as magnetic anomaly. One can explain the anomalously large fields measured at altitude (>100 km) by appealing to rock that is intrinsically intensely magnetized (e.g., few 100 A/m) and/or by requiring that the scale length of coherent magnetization be comparable to the altitude of observation (e.g., 100 km). These possibilities are not exclusive, i.e., one may also appeal to both: intensely magnetized rock, magnetized with a coherence scale length measured in many tens, or

hundreds, of km. This is an argument put forth by (Connerney et al., 2005; Connerney et al., 1999) in their discussion of the possibility of plate tectonics on early Mars.

An acquisition of magnetic remanence needs to consider a lateral distribution of the secondary magnetic field generated by crustal remanent sources containing magnetic carriers of certain grain size and mineralogy. Such magnetic source is able to produce an ambient magnetic field of larger intensity than preexisting dynamo (Kletetschka et al., 2005). This ambient field is capable of magnetizing portions of deeper crust that cools through its blocking temperatures in an absence of dynamo. Analysis of magnetization of magnetic minerals of various grain size and concentration reveals that magnetite grains less than 0.01mm in size, and hematite grains larger than 0.01mm in size can become effective magnetic source capable of magnetizing magnetic minerals contained in surrounding volume. Preexisting crustal remanence (for example ~250 A/m relates to 25% of multi-domain hematite, see (Kletetschka et al., 2000)) can trigger a self-magnetizing process that can continue in the absence of magnetic dynamo and continue strengthening and/or weakening magnetic anomalies on Mars. Thickness of the primary magnetic layer and concentration of magnetic carriers allow specification of the temperature gradient required to trigger a self-magnetization process (Kletetschka et al., 2005).

The appeal to intensely magnetized rock motivates our analysis of magnetic minerals with high aspect ratio. If such minerals are present within the Mars crust, they would inherit a larger magnetic coercivity. There is some evidence that the more intense magnetic anomalies consist of magnetic material of higher coercivity based on distribution of magnetic anomalies near impact craters (Kletetschka et al., 2004b) and magnetic anomaly modeling (Shahnas and Arkani-Hamed, 2007). Therefore we suggest that magnetic anomalies on Mars may have acquired anomalously intense magnetization by virtue of separation of magnetic minerals from the silicate in the forms of continuous bands (gneiss texture). Such a magnetic fabric may occur during the formation of the secondary crust (Taylor, 1992; Taylor et al., 2006) by partial melting of the interior. This is similar to the effect of highly deformed rock from India.

Another effect to enhance the efficiency of remanent magnetization is the following. Theoretical considerations and detailed modeling (Elkins-Tanton et al., 2003) indicate that Al will be sequestered in the mantle, depleting the residual magma ocean in Al, and leading to delayed plagioclase nucleation. Such a delay would lead to precipitation of iron oxides within the plagioclases with the preferred planes defined by the plagioclase crystallography (Frost and Lindsley, 1991). This process could lead to the magnetization enhancement observed in Archean anorthosite (Figure 3).

Our previous work (Kletetschka, 2000; Kletetschka et al., 2004a) emphasized that efficiency of acquisition of magnetic remanence is an important factor when analyzing magnetic anomalies due to remanence. We identified that hematite/titanohematite can be an important candidate for generation of Mars magnetic anomalies. In this work we identified magnetic anisotropy of magnetic carriers and textural patterns of the crustal rocks are another important contributing factors that may generate a coherent patterns of planetary magnetic anomalies.

The slightly lower FeO content of the southern highlands compared to the northern plains (Taylor et al., 2006) may be the result of southern highland basalts being derived from, on average, shallower depths than those of the northern plains. Thus the

residual melt may have crystallized largely in place, perhaps in large part by local equilibrium crystallization leading to local extensive density separation forming distinctive bands. Our analysis indicates that such bands can significantly enhance the overall TRM magnetization per unit volume. This could lead to large magnetic anomalies over the regions that experienced a large degree of density differentiation (i.e. gneiss rock type formed) passively associated with the massive sinking of the lower crust and mantle towards the core during the first 100 million years (Yokochi and Marty, 2005). Due to large scale of such massive mass motion it is possible that such mechanism may be consistent with the large-scale length of coherent magnetization differences.

We interpret that the presence of strong magnetic anomalies is likely to be associated with density segregation within the deep crust. Density segregation has occurred and is occurring in terrestrial environment as part of the crustal evolution. On planet Earth the presence of the global magnetic field prevents observation of remanent dominated magnetic anomalies that may be associated with such anisotropic textures. Density segregation was likely to occur on Mars and therefore allowed for formation of anisotropic textures, similar to terrestrial, in deep crustal environment. Such analogy is consistent with formation of enhanced magnetic remanence due to anisotropy leading to the origin of magnetic anomalies on Mars.

Constraints for plate motion mechanisms:

A number of driving forces have been proposed to participate in driving terrestrial plate tectonics including ridge push, slab pull, trench suction, collisional resistance and basal drag. Until recently, most models were based on plate and boundary forces like ridge push and subduction pull (Bott, 1990; Stefanick and Jurdy, 1992). However, (Ziegler, 1992) showed that plate motion during the Phanerozoic rules out the boundary forces during certain periods of tectonic development. Ziegler suggested that the asthenosphere, as a part of a large scale convection cycle, acts by its horizontal shear traction on the base of the lithosphere. This is supported by convection modeling (Quere and Forte, 2006). This convection style generates a force, which dominates in a plate driving mechanism, at least during the continental break-up and initiation of new subduction systems. There the contribution to the shear traction will depend whether the mantle pattern below is unidirectional or radial (Doglioni, 1993; Pavoni, 1993).

The evolution of both the African continent and the Pacific plate suggests a bicellular mantle circulation system in Earth constraining the two major superplumes regions, one below Africa and one below the Pacific plate (Pavoni, 1993). A downwelling zone associated with the bicellular system forms a great circle along North and South America, through Antarctica, Australia and Asia and back to North America. Another independent observation supporting the position of both superplumes is the temperature distribution near the mantle core boundary (Cadek et al., 1994; Yuen et al., 1994) based on tomographic data (Morelli and Dziewonski, 1987) and numerical model (Yuen et al., 1993). This modeling suggests that the radial transfer of heat and mass from the core-mantle boundary to the surface occurred in a radial direction from the core rather than laterally away from the plume initiation.

With this in mind one may explain the intensely magnetized southern highlands (Figure 1) in terms of the high coercivity signature associated (zone 3) with crustal differentiation and deformation of the crustal material above the downwelling mantle. Such deformation would be passive, related to the unicellular pattern of convection similar in analogy as was proposed for bicellular terrestrial convection pattern (Ziegler, 1992). This proposal is illustrated in Figure 6, where we show the presence of intense magnetic anomalies on Mars above the location of the down-welling zone formed during the early planetary differentiation phase. Such initial distribution of magnetic anomalies would be modified further by demagnetization events due to large impacts (E.g. Hellas, Argyre, Prometheus) and formation of volcanic provinces (Tharsis, Illisium) at the absence of global magnetic field (Acuna et al., 1999; Connerney et al., 2001).

Our unicellular model suggests antipods of upwelling and downwelling zones. The strongest magnetic anomalies on Mars are centered near 50S latitude and 180E longitude (Figure 1). The northern owlands are centered at roughly 60N and 180E. These two regions are therefore separated by about 110 degrees and are not exactly opposite to one another as would be expected according to our idealized model (Figure 6). This is because the upwelling and downelling zones are not necessarily symmetrical as each may be a cluster of multiple upwelling and downwelling zones. For this reason they may not necessarily be exactly opposite to each other (see also references to the numerical convection models (Breuer et al., 1993; Yuen et al., 1993; Yuen et al., 1994)).

Conclusions

We propose that Mars may have experienced a simple uni-cellular convection cell similar to the bicellular convection proposed for earth, where two upwelling zones are located under Africa and the Pacific, with down welling of dense material descending under the buoyant roots of continental plates (Ziegler, 1992). Indirect evidence of density segregation under the area of intense magnetic anomalies on Mars suggests that denser material may have been pulled down into an area of elevated pressure and temperature. Less dense rock rich in silicates is less viscous and flows upward along the lithic bands leaving behind mafic iron rich volumes. Such thin plates give rise to a very efficient capacity to acquire thermal remanent magnetization due to lower demagnetizing factor of elongated magnetic carriers. During the magnetizing process, we may need to consider self-magnetization (Kletetschka et al., 2005) due to large concentration of iron rich minerals (Taylor et al., 2006), which may further contribute to the magnetic anomalies observed by the Mars Global Surveyor mission in Zone 3 (Figure 1).

Our TRM measurements, both on minerals with high aspect ratio and magnetic minerals segregated into bands, indicate significantly more effective acquisition of thermal remanence as dictated by associated lower demagnetizing field. Based on these observations we suggest the following model explaining both the Martian dichotomy as well as distribution of magnetic anomalies on Mars. Mars forms an early primary crust with the mantle differentiating according to consistent convection models (Breuer et al., 1993; Van Thienen et al., 2006). The down-welling zone near the South Pole causes rock differentiation into silicate rich buoyant rock with low viscosity. The low density rock forms the crust and as it cools it acquires remanent magnetization. With time the crust

made of lower density rock accumulates around the South Pole and starts to form a dichotomy in a way similar to Earth. Dense gabbroic rock forms low lands and a relatively thin crust. Lower density rock (diorite, anorthosite) will form lighter volumes that will float on the dense rock and form a continent-like block. This continent grows rapidly and an area of subduction is formed along the continent boundary. An active dynamo magnetizes the crust as it cools below the blocking temperatures of the magnetic minerals. This dynamo may be reversing causing different blocks to magnetize in reversed direction. As the convection in the core stops, the dynamo stops as well. Subsequent large meteorite impacts and volcanic provinces demagnetize portions of the Mars crust. The region above the down-welling zone contains intense magnetic anomalies due to large anisotropy of stretched and deformed rocks.

Figure Captions:

Figure 1: Three main zones containing magnetic field with low to negligible (Zone 1), intermediate (Zone 2), and large (Zone 3) magnetic intensities. Magnetic map shows radial component (B_r) of the magnetic field measured on the night side of Mars and is taken from Connerney et al., (2001). Labels Hellas, Prometheus, Agyre, and Isidis indicate approximate locations of these impact craters.

Figure 2: Top: crustal magnetic field magnitude at 195 km altitude from electron reflectometry (Lillis et al., 2006; Mitchell et al., 2005). Closed magnetic field regions at ~ satellite magnetic mapping altitude 400 km, where electron reflectometry is not possible, are represented by black. The white circle near the south pole is the 860 km-diameter Prometheus impact basin. Moving east from the basin center, crustal field intensity changes by >2 orders of magnitude over ~500 km. Bottom: same region but magnetic data (along–track derivative of the radial component are at 400 km magnetic mapping altitude (Connerney et al., 2005).

Figure 3: Magnetic characterization of oxide needles within anorthosite (modified from Kletetschka et al, 2006). A. The stability of saturation remanence given at 295 K in 5 T is monitored during the low temperature cycle. The magnetization transition at 120 K (Verwey transition) is characteristic of magnetite. B. Thermal remanence acquisition (at 0.05 mT) normalized by saturation remanence (SIRM) of anorthosite oxide needles (1/50 aspect ratio SD M) is compared with acquisition of equi-dimensional multidomain, pseudosingle domain, and single domain magnetite grains (Kletetschka et al., 2006; Yu, 2007)

Figure 4: Sample numbers 1, 2, 3 and 4 represent adjacent pairs of metamorphic rock specimens where within each pair there are rock samples with and without significant elongation. (a) Images of the textures of metamorphic Kohistan samples. Top images are with the stretched fabric and represent smaller demagnetizing field than would be in bottom images where there is small or no fabric. Width of the images is 0.5 mm. See the text for more information. (b) Measurements of efficiency of Thermoremanent magnetization. The samples identified as “fabric” contain mafic bands stretched approximately to 1:6 aspect ratio. “No fabric” minerals were relatively homogeneous with no obvious anisotropy between mafic and lithic grains. (c) Approximation of the TRM/SIRM multiplication factor due to aspect ratio (width/length) variation based on Kletetschka et al., 2004, 2006 and Yu, 2007 data.

Figure 5: 2D model of intense magnetic anomalies of Mars crust. Individual magnetizing elements are 50x50 km in size and anti-parallel oriented (up and down as shown by white arrows). Blocks with denser field lines have magnetization 300 A/m corresponding to elongated grains of magnetite. The rest of the blocks have magnetization 60 A/m. These magnetizations generate comparable magnetic intensity as detected by Magnetometer on board of Mars Global Surveyor at 400 km as well as by reflected electrons at 190 km (see black dashed lines).

Figure 6: Cartoon of hypothesized convection pattern of mantle moving relative to the core. Mantle is driven by thermal energy and causes passive motion and deformation of the crust resulting in dichotomy between the low- and high-density crust (northern low-lands and southern highlands, respectively). Such convection allows formation of three magnetic zones: Zone 1- low to no magnetic anomalies, Zone 2 – medium magnetic anomalies, Zone 3 – high magnetic anomalies.

References:

ACUNA M. H., CONNERNEY J. E. P., NESS N. F., LIN R. P., MITCHELL D., CARLSON C. W., MCFADDEN J., ANDERSON K. A., REME H., MAZELLE C., VIGNES D., WASILEWSKI P. and CLOUTIER P. (1999) Global distribution of crustal magnetization discovered by the Mars Global Surveyor MAG/ER experiment. *Science* **284**(5415), 790-793.

ARKANI-HAMED J. (2002) Magnetization of the Martian crust. *Journal of Geophysical Research* **107**(E5), doi:10.1029/2001JE001496.

BARD J. P. (1983) Metamorphism Of An Obducted Island-Arc - Example Of The Kohistan Sequence (Pakistan) In The Himalayan Collided Range. *Earth And Planetary Science Letters* **65**(1), 133-144.

BOTT M. H. P. (1990) Stress-Distribution And Plate Boundary Force Associated With Collision Mountain-Ranges. *Tectonophysics* **182**(3-4), 193-209.

BREUER D., SPOHN T. and WULLNER U. (1993) Mantle Differentiation And The Crustal Dichotomy Of Mars. *Planetary And Space Science* **41**(4), 269-283.

CADEK O., YUEN D. A., STEINBACH V., CHOPELAS A. and MATYSKA C. (1994) Lower Mantle Thermal Structure Deduced From Seismic Tomography, Mineral Physics And Numerical Modeling. *Earth And Planetary Science Letters* **121**(3-4), 385-402.

CONNERNEY J. E. P., ACUNA M. H., NESS N. F., KLETETSCHKA G., MITCHELL D. L., LIN R. P. and REME H. (2005) Tectonic implications of Mars crustal magnetism. *Proceedings Of The National Academy Of Sciences Of The United States Of America* **102**(42), 14970-14975.

CONNERNEY J. E. P., ACUNA M. H., NESS N. F., SPOHN T. and SCHUBERT G. (2004) Mars crustal magnetism. *Space Science Reviews* **111**(1-2), 1-32.

CONNERNEY J. E. P., ACUNA M. H., WASILEWSKI P. J., KLETETSCHKA G., NESS N. F., REME H., LIN R. P. and MITCHELL D. L. (2001) The global magnetic field of Mars and implications for crustal evolution. *Geophysical Research Letters* **28**(21), 4015-4018.

CONNERNEY J. E. P., ACUñA M. H., WASILEWSKI P. J., NESS N. F., REME H., MAZELLE C., VIGNES D., LIN R. P., MITCHELL D. L. and CLOUTIER P. A. (1999) Magnetic Lineations in the Ancient Crust of Mars. *Science* **284**, 794-798.

DOGLIONI C. (1993) Geological Evidence For A Global Tectonic Polarity. *Journal Of The Geological Society* **150**, 991-1002.

DUNLOP D. J. and ÖZDEMIR Ö. (1997) *Rock magnetism: fundamentals and frontiers*. Cambridge University Press, Cambridge. pp. 573.

ELKINS-TANTON L. T., PARMENTIER E. M. and HESS P. C. (2003) Magma ocean fractional crystallization and cumulate overturn in terrestrial planets: Implications for Mars. *Meteorit. Planet. Sci.* **38**, 1753-1771.

FROST B. R. and LINDSLEY D. H. (1991) Occurence of Iron-Titanium Oxides in Igneous Rocks. In *Oxides Minerals: Petrologic and Magnetic Significance* (ed. D. H. Lindsley), pp. 433-468. Mineralogical Society of America, Blacksburg.

KLETETSCHKA G. (2000) Intense remanence of hematite-ilmenite solid solution. *Geologica Carpathica* **51**(3), 187-187.

KLETETSCHKA G., ACUNA M. H., KOHOUT T., WASILEWSKI P. J. and CONNERNEY J. E. P. (2004a) An empirical scaling law for acquisition of thermoremanent magnetization. *Earth And Planetary Science Letters* **226**(3-4), 521-528.

KLETETSCHKA G., CONNERNEY J. E. P., NESS N. F. and ACUNA M. H. (2004b) Pressure effects on martian crustal magnetization near large impact basins. *Meteoritics & Planetary Science* **39**(11), 1839-1848.

KLETETSCHKA G., FULLER M. D., KOHOUT T., WASILEWSKI P. J., HERRERO-BERVERA E., NESS N. F. and ACUNA M. H. (2006) TRM in low magnetic fields: a minimum field that can be recorded by large multidomain grains. *Physics Of The Earth And Planetary Interiors* **154**(3-4), 290-298.

KLETETSCHKA G., NESS N. F., CONNERNEY J. E. P., ACUNA M. H. and WASILEWSKI P. J. (2005) Grain size dependent potential for self generation of magnetic anomalies on Mars via thermoremanent magnetic acquisition and magnetic interaction of hematite and magnetite. *Physics Of The Earth And Planetary Interiors* **148**(2-4), 149-156.

KLETETSCHKA G., WASILEWSKI P. J. and TAYLOR P. T. (2000) Mineralogy of the sources for magnetic anomalies on Mars. *Meteoritics & Planetary Science* **35**(5), 895-899.

LILLIS R. J., MANGA M., MITCHELL D. L., LIN R. P. and ACUNA M. H. (2006) Unusual magnetic signature of the Hadriaca Patera volcano: Implications for early Mars. *Geophysical Research Letters* **33**(3).

LOUZADA K. L., STEWART S. T. and WEISS B. P. (2007) Effect of shock on the magnetic properties of pyrrhotite, the Martian crust, and meteorites. *Geophysical Research Letters* **34**(5).

MITCHELL D. L., LILLIS R. J., LIN R. P., CONNERNEY J. E. P. and ACUNA M. H. (2005) A Global Map of Mars' Crustal Magnetic Field Based on Electron Reflectometry. In *Lunar and Planetary Science XXXVI*, pp. 2366.pdf. Lunar and Planetary Institute, Houston, Texas.

MOHIT P. S. and ARKANI-HAMED J. (2004) Impact demagnetization of the martian crust. *Icarus* **168**(2), 305-317.

MORELLI A. and DZIEWONSKI A. M. (1987) Topography Of The Core-Mantle Boundary And Lateral Homogeneity Of The Liquid Core. *Nature* **325**(6106), 678-683.

NEUMANN G. A., ZUBER M. T., WIECZOREK M. A., MCGOVERN P. J., LEMOINE F. G. and SMITH D. E. (2004) Crustal structure of Mars from gravity and topography. *Journal Of Geophysical Research-Planets* **109**(E8).

NIMMO F. and GILMORE M. S. (2001) Constraints on the depth of magnetized crust on Mars from impact craters. *Journal of Geophysical Research-Planets* **106**(E6), 12315-12323.

PAVONI N. (1993) Pattern Of Mantle Convection And Pangaea Break-Up, As Revealed By The Evolution Of The African Plate. *Journal Of The Geological Society* **150**, 953-964.

QUERE S. and FORTE A. M. (2006) Influence of past and present-day plate motions on spherical models of mantle convection: implications for mantle plumes and hotspots. *Geophysical Journal International* **165**(3), 1041-1057.

QUESNEL Y., LANGLAIS B. and SOTIN C. (2007) Local inversion of magnetic anomalies: Implication for Mars' crustal evolution. *Planetary And Space Science* **55**(3), 258-269.

RASMUSSEN H., GUNNLAUGSSON H. P., TEGNER C. and KRISTJANSSON L. (2006) Magnetic properties of Martian olivine basalts studied by terrestrial analogues. *Hyperfine Interactions* **166**(1-4), 561-566.

ROCHETTE P., FILLION G., BALLOU R., BRUNET F., OULADDIAF B. and HOOD L. (2003) High pressure magnetic transition in pyrrhotite and impact demagnetization on Mars. *Geophysical Research Letters* **30**(13).

SCHLINGER C. M., KHAN M. J. and WASILEWSKI P. (1989) Rock Magnetism of the Kohistan Island Arc, Pakistan. In *Geol. Bull. Univ. Peshawar*, pp. 83-101.

SCHUBERT G., RUSSELL C. T. and MOORE W. B. (2000) Geophysics - Timing of the Martian dynamo. *Nature* **408**(6813), 666-667.

SCOTT E. R. D. and FULLER M. (2004) A possible source for the Martian crustal magnetic field. *Earth And Planetary Science Letters* **220**(1-2), 83-90.

SELKIN P. A., GEE J. S., TAUXE L., MEURER W. P. and NEWELL A. J. (2000) The effect of remanence anisotropy on paleointensity estimates: a case study from the Archean Stillwater Complex. *Earth And Planetary Science Letters* **183**(3-4), 403-416.

SHAHNAS H. and ARKANI-HAMED J. (2007) Viscous and impact demagnetization of Martian crust. *Journal Of Geophysical Research-Planets* **112**(E2).

STEFANICK M. and JURDY D. M. (1992) Stress Observations And Driving Force Models For The South-American Plate. *Journal Of Geophysical Research-Solid Earth* **97**(B8), 11905-11913.

STEVENSON D. J., SPOHN T. and SCHUBERT G. (1983) Magnetism And Thermal Evolution Of The Terrestrial Planets. *Icarus* **54**(3), 466-489.

TAYLOR G. J. (1992) *Solar System Evolution: A New Perspective*. Univ. Press., New York. pp. 307.

TAYLOR G. J., BOYNTON W., BRUCKNER J., WANKE H., DREIBUS G., KERRY K., KELLER J., REEDY R., EVANS L., STARR R., SQUYRES S., KARUNATILLAKE S., GASNAULT O., MAURICE S., D'USTON C., ENGLERT P., DOHM J., BAKER V., HAMARA D., JANES D., SPRAGUE A., KIM K. and DRAKE D. (2006) Bulk composition and early differentiation of Mars. *Journal Of Geophysical Research-Planets* **111**(E3).

VAN THIENEN P., RIVOLDINI A., VAN HOOLST T. and LOGNONNE P. (2006) A top-down origin for martian mantle plumes. *Icarus* **185**(1), 197-210.

VERWEY E. J., HAAYMAN P. W. and ROMEIJN F. C. (1947) Physical properties and cation arrangements of oxides with spinel structure. *J. Chem. Phys.* **15**, 181-187.

XU W. X., GEISSMAN J. W., VANDERVOO R. and PEACOR D. R. (1997) Electron microscopy of iron oxides and implications for the origin of magnetizations and rock magnetic properties of Banded Series rocks of the Stillwater Complex, Montana. *Journal Of Geophysical Research-Solid Earth* **102**(B6), 12139-12157.

YOKOCHI R. and MARTY B. (2005) Geochemical constraints on mantle dynamics in the Hadean. *Earth And Planetary Science Letters* **238**(1-2), 17-30.
YU Y. (2007) A linear field dependence of thermoremanence in low magnetic fields. *Physics Of The Earth And Planetary Interiors* **162**, 244-248.
YU Y. J. (2006) How accurately can NRM/SIRM determine the ancient planetary magnetic field intensity? *Earth And Planetary Science Letters* **250**(1-2), 27-37.
YUEN D. A., CADEK O., CHOPELAS A. and MATYSKA C. (1993) Geophysical Inferences Of Thermal-Chemical Structures In The Lower Mantle. *Geophysical Research Letters* **20**(10), 899-902.
YUEN D. A., CADEK O. P., BOEHLER R., MOSER J. and MATYSKA C. (1994) Large Cold Anomalies In The Deep Mantle And Mantle Instability In The Cretaceous. *Terra Nova* **6**(3), 238-245.
ZIEGLER P. A. (1992) Plate-Tectonics, Plate Moving Mechanisms And Rifting. *Tectonophysics* **215**(1-2), 9-34.

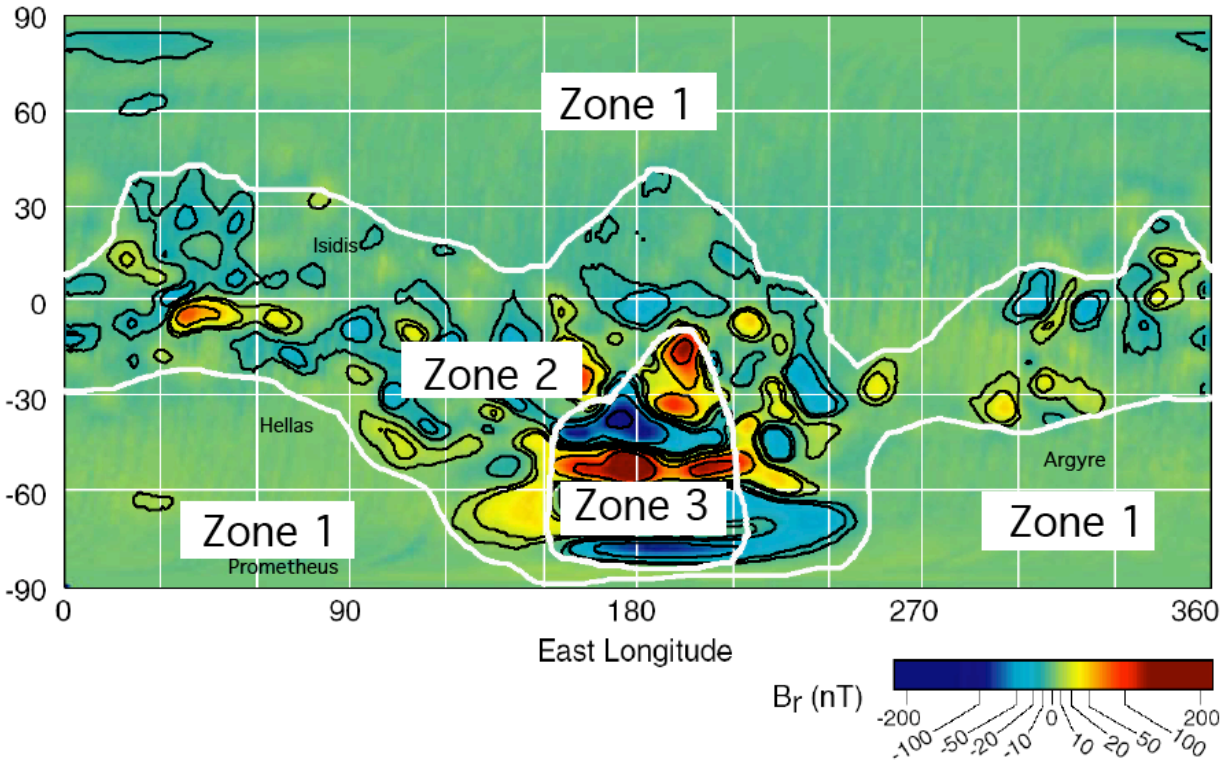

Figure 1: Three main zones containing magnetic field with low to negligible (Zone 1), intermediate (Zone 2), and large (Zone 3) magnetic intensities. Magnetic map shows radial component (B_r) of the magnetic field measured on the night side of Mars and is taken from Connerney et al., (2001). Labels Hellas, Prometheus, Agyre, and Isidis indicate approximate locations of these impact craters.

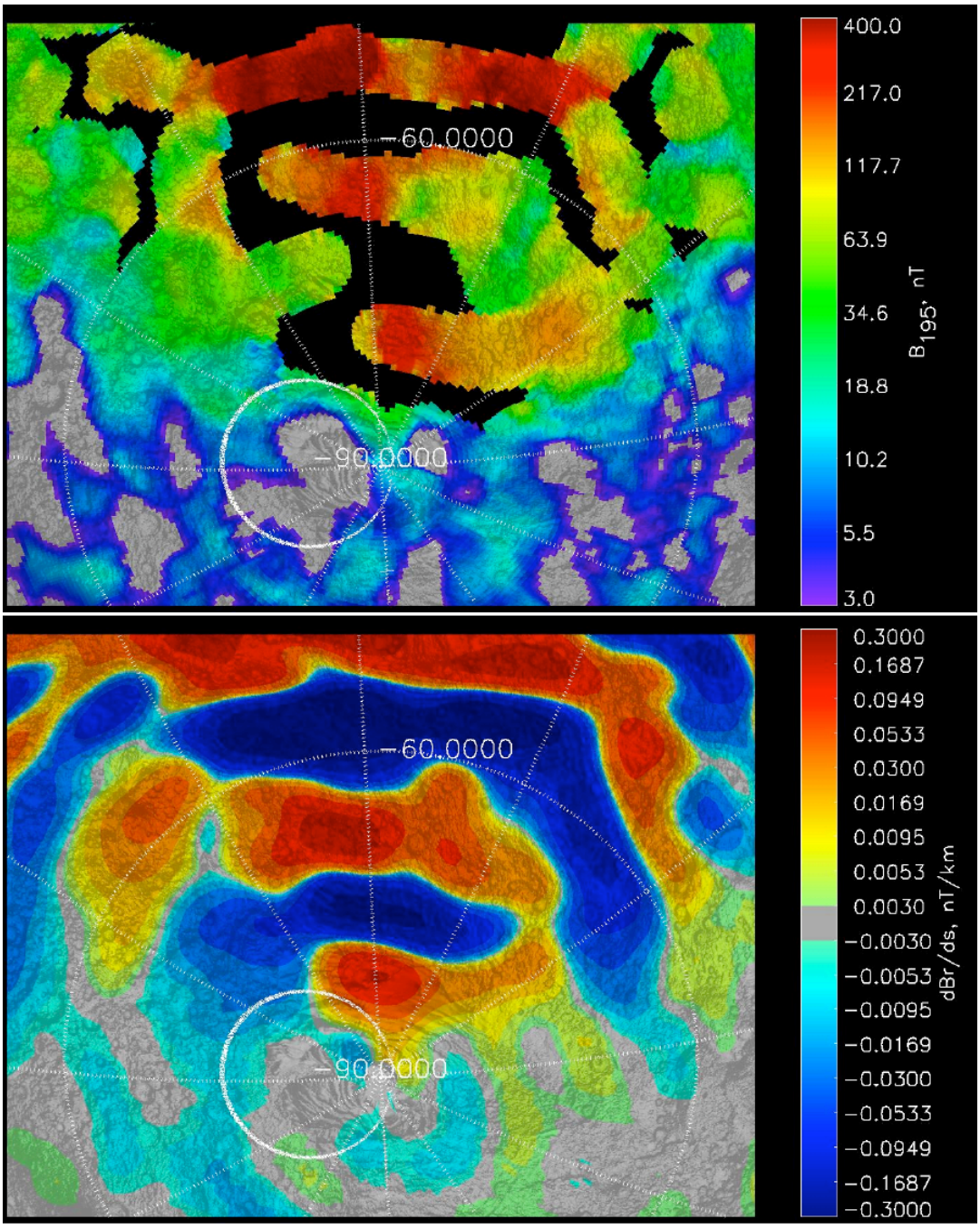

Figure 2: Top: crustal magnetic field magnitude at 195 km altitude from electron reflectometry (Lillis et al., 2006; Mitchell et al., 2005). Closed magnetic field regions at ~ satellite magnetic mapping altitude 400 km, where electron reflectometry is not possible, are represented by black. The white circle near the south pole is the 860 km-diameter Prometheus impact basin. Moving east from the basin center, crustal field intensity changes by >2 orders of magnitude over ~500 km. Bottom: same region but magnetic data (along–track derivative of the radial component are at 400 km magnetic mapping altitude (Connerney et al., 2005).

.

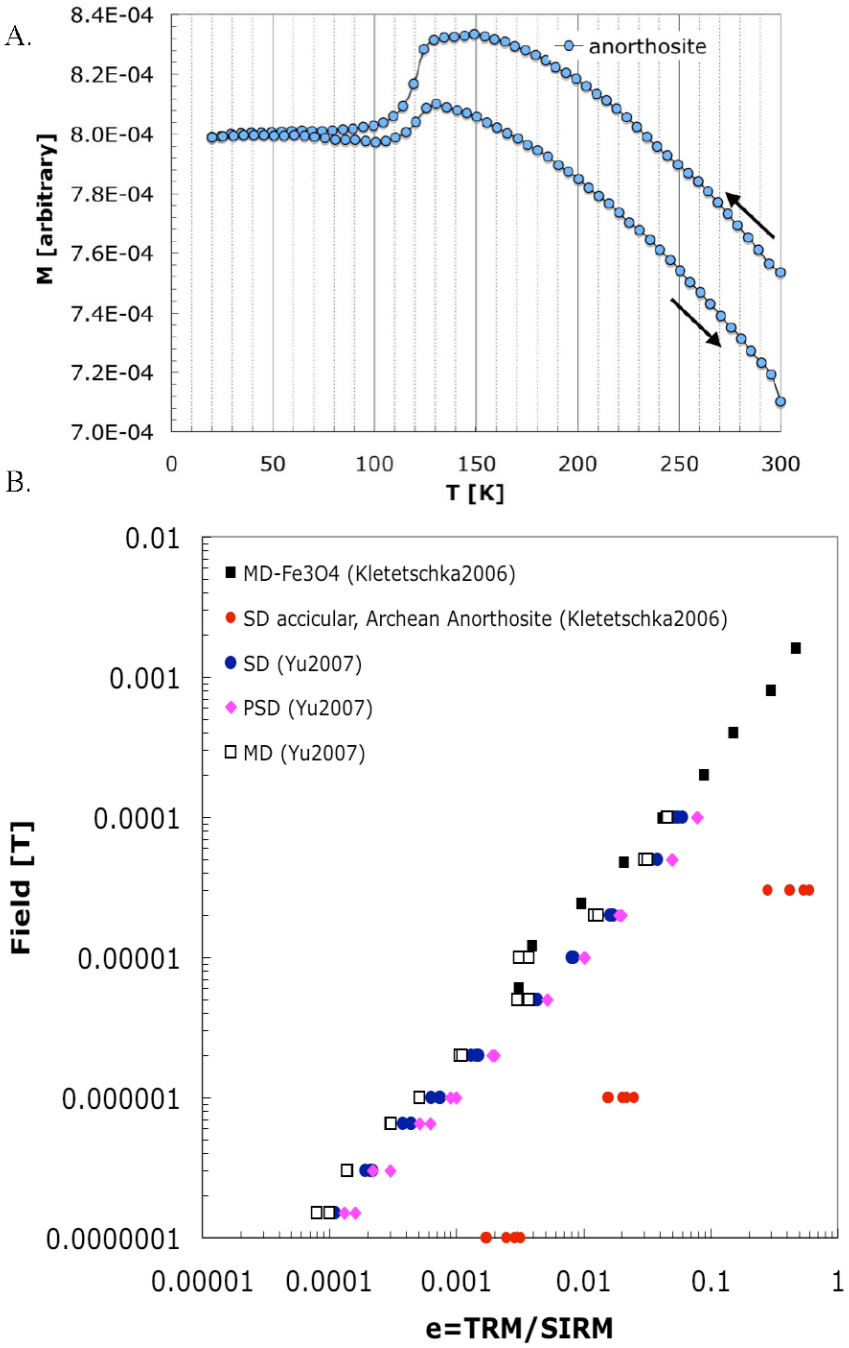

Figure 3: Magnetic characterization of oxide needles within anorthosite (modified from Kletetschka et al, 2006). A. The stability of saturation remanence given at 295 K in 5 T is monitored during the low temperature cycle. The magnetization transition at 120 K (Verwey transition) is characteristic of magnetite. B. Thermal remanence acquisition (at 0.05 mT) normalized by saturation remanence (SIRM) of anorthosite oxide needles (1/50 aspect ratio SD M) is compared with acquisition of equi-dimensional multidomain, pseudosingle domain, and single domain magnetite grains (Kletetschka et al., 2006; Yu, 2007)

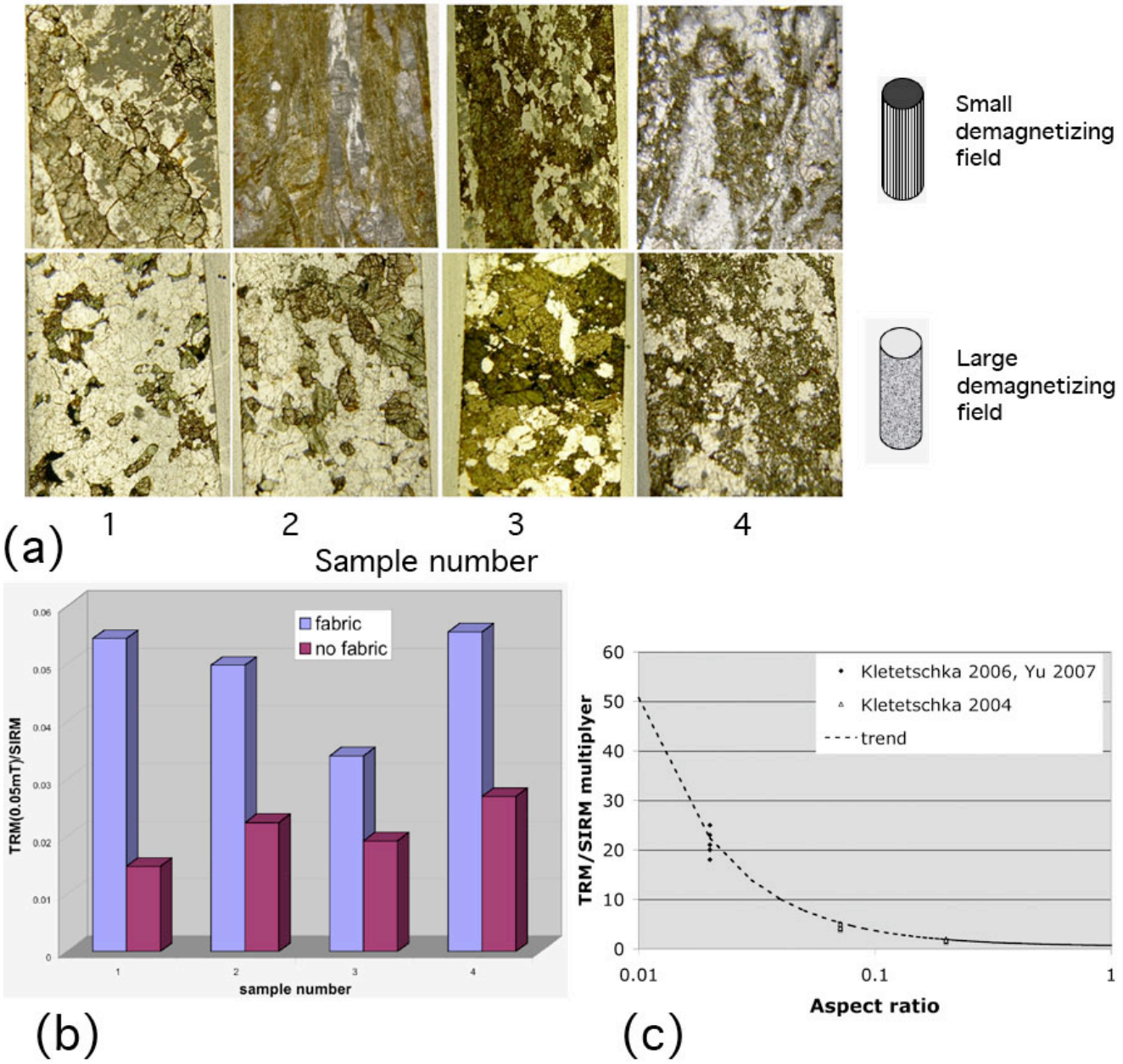

Figure 4: Sample numbers 1, 2, 3 and 4 represent adjacent pairs of metamorphic rock specimens where within each pair there are rock samples with and without significant elongation. (a) Images of the textures of metamorphic Kohistan samples. Top images are with the stretched fabric and represent smaller demagnetizing field than would be in bottom images where there is small or no fabric. Width of the images is 0.5 mm. See the text for more information. (b) Measurements of efficiency of Thermoremanent magnetization. The samples identified as "fabric" contain mafic bands stretched approximately to 1:6 aspect ratio. "No fabric" minerals were relatively homogeneous with no obvious anisotropy between mafic and lithic grains. (c) Approximation of the TRM/SIRM multiplication factor due to aspect ratio (width/length) variation based on Kletetschka et al., 2004, 2006 and Yu, 2007 data.

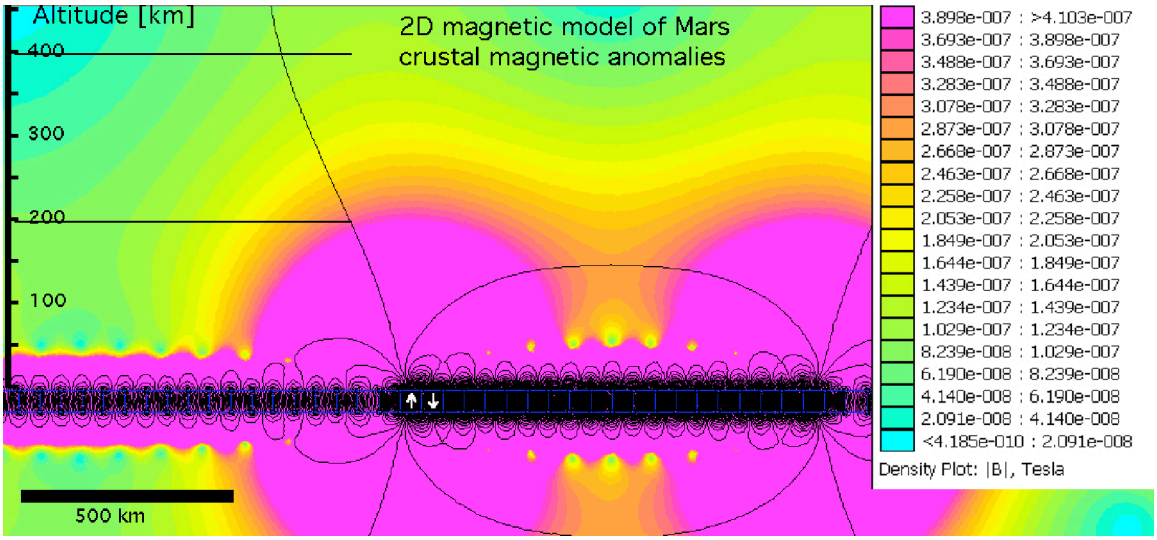

Figure 5: 2D model of intense magnetic anomalies of Mars crust. Individual magnetizing elements are 50x50 km in size and anti-parallel oriented (up and down as shown by white arrows). Blocks with denser field lines have magnetization 300 A/m corresponding to elongated grains of magnetite. The rest of the blocks have magnetization 60 A/m. These magnetizations generate comparable magnetic intensity as detected by Magnetometer on board of Mars Global Surveyor at 400 km as well as by reflected electrons at 190 km (see black dashed lines).

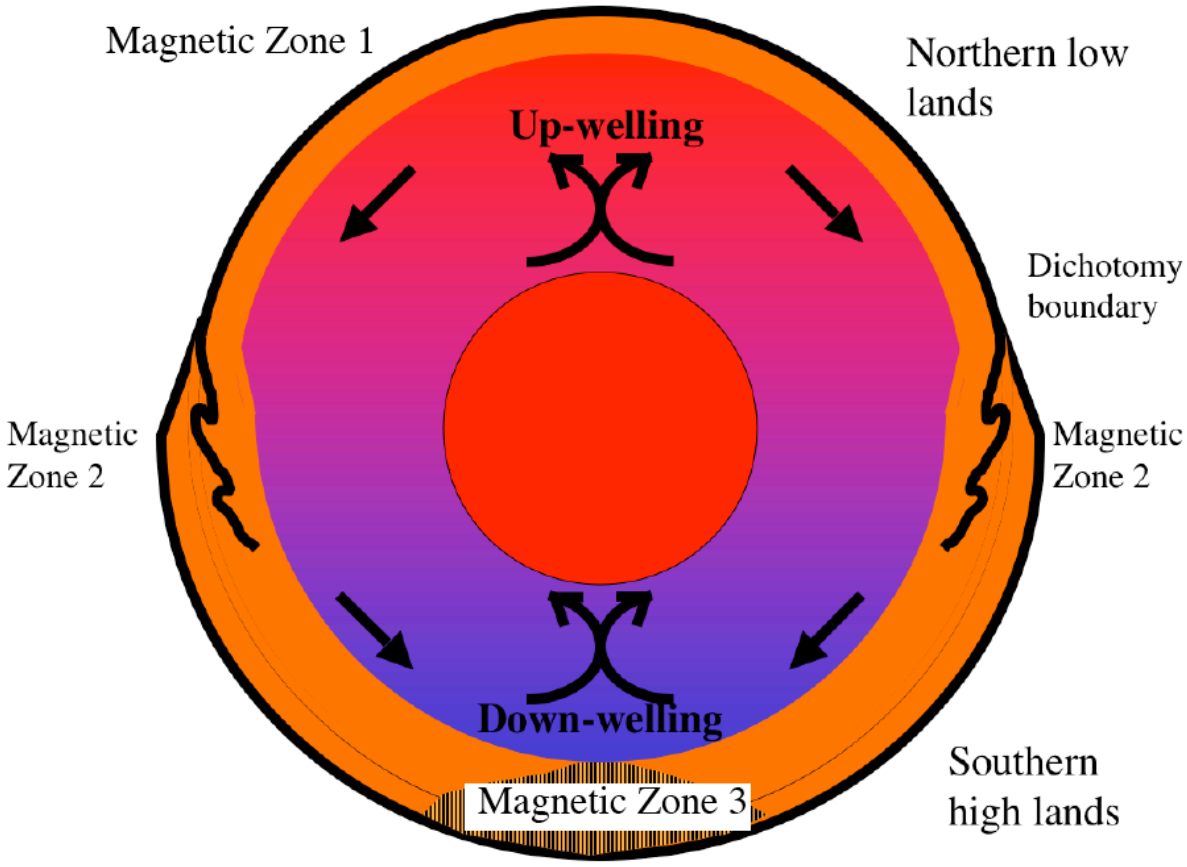

Figure 6: Cartoon of hypothesized convection pattern of mantle moving relative to the core. Mantle is driven by thermal energy and causes passive motion and deformation of the crust resulting in dichotomy between the low- and high-density crust (northern low-lands and southern highlands, respectively). Such convection allows formation of three magnetic zones: Zone 1- low to no magnetic anomalies, Zone 2 – medium magnetic anomalies, Zone 3 – high magnetic anomalies.